

Observation of the decay $B_s^0 \rightarrow J/\psi\eta$ and Evidence for $B_s^0 \rightarrow J/\psi\eta'$

I. Adachi,¹⁰ H. Aihara,⁵⁹ K. Arinstein,^{1,41} T. Aso,⁶³ V. Aulchenko,^{1,41} T. Aushev,^{26,19} T. Aziz,⁵⁴ S. Bahinipati,³ A. M. Bakich,⁵³ V. Balagura,¹⁹ Y. Ban,⁴⁵ E. Barberio,³⁰ A. Bay,²⁶ I. Bedny,^{1,41} K. Belous,¹⁶ V. Bhardwaj,⁴⁴ B. Bhuyan,¹³ M. Bischofberger,³³ S. Blyth,³⁵ A. Bondar,^{1,41} A. Bozek,³⁷ M. Bračko,^{28,20} J. Brodzicka,³⁷ T. E. Browder,⁹ M.-C. Chang,⁴ P. Chang,³⁶ Y.-W. Chang,³⁶ Y. Chao,³⁶ A. Chen,³⁴ K.-F. Chen,³⁶ P.-Y. Chen,³⁶ B. G. Cheon,⁸ C.-C. Chiang,³⁶ R. Chistov,¹⁹ I.-S. Cho,⁶⁵ S.-K. Choi,⁷ Y. Choi,⁵² J. Crnkovic,¹² J. Dalseno,^{29,55} M. Danilov,¹⁹ A. Das,⁵⁴ M. Dash,⁶⁴ A. Drutskoy,³ W. Dungen,¹⁵ S. Eidelman,^{1,41} D. Epifanov,^{1,41} M. Feindt,²² H. Fujii,¹⁰ M. Fujikawa,³³ N. Gabyshev,^{1,41} A. Garmash,^{1,41} G. Gokhroo,⁵⁴ P. Goldenzweig,³ B. Golob,^{27,20} M. Grosse Perdekamp,^{12,47} H. Guo,⁴⁹ H. Ha,²³ J. Haba,¹⁰ B.-Y. Han,²³ K. Hara,³¹ T. Hara,¹⁰ Y. Hasegawa,⁵¹ N. C. Hastings,⁵⁹ K. Hayasaka,³¹ H. Hayashii,³³ M. Hazumi,¹⁰ D. Heffernan,⁴³ T. Higuchi,¹⁰ Y. Horii,⁵⁸ Y. Hoshi,⁵⁷ K. Hoshina,⁶² W.-S. Hou,³⁶ Y. B. Hsiung,³⁶ H. J. Hyun,²⁵ Y. Igarashi,¹⁰ T. Iijima,³¹ K. Inami,³¹ A. Ishikawa,⁴⁸ H. Ishino,^{60,*} K. Itoh,⁵⁹ R. Itoh,¹⁰ M. Iwabuchi,⁶ M. Iwasaki,⁵⁹ Y. Iwasaki,¹⁰ T. Jinno,³¹ M. Jones,⁹ N. J. Joshi,⁵⁴ T. Julius,³⁰ D. H. Kah,²⁵ H. Kakuno,⁵⁹ J. H. Kang,⁶⁵ P. Kapusta,³⁷ S. U. Kataoka,³² N. Katayama,¹⁰ H. Kawai,² T. Kawasaki,³⁹ A. Kibayashi,¹⁰ H. Kichimi,¹⁰ C. Kiesling,²⁹ H. J. Kim,²⁵ H. O. Kim,²⁵ J. H. Kim,⁵² S. K. Kim,⁵⁰ Y. I. Kim,²⁵ Y. J. Kim,⁶ K. Kinoshita,³ B. R. Ko,²³ S. Korpar,^{28,20} M. Kreps,²² P. Križan,^{27,20} P. Krokovny,¹⁰ T. Kuhr,²² R. Kumar,⁴⁴ T. Kumita,⁶¹ E. Kurihara,² E. Kuroda,⁶¹ Y. Kuroki,⁴³ A. Kusaka,⁵⁹ A. Kuzmin,^{1,41} Y.-J. Kwon,⁶⁵ S.-H. Kyeong,⁶⁵ J. S. Lange,⁵ G. Leder,¹⁵ M. J. Lee,⁵⁰ S. E. Lee,⁵⁰ S.-H. Lee,²³ J. Li,⁹ A. Limosani,³⁰ S.-W. Lin,³⁶ C. Liu,⁴⁹ D. Liventsev,¹⁹ R. Louvot,²⁶ J. MacNaughton,¹⁰ F. Mandl,¹⁵ D. Marlow,⁴⁶ A. Matyja,³⁷ S. McOnie,⁵³ T. Medvedeva,¹⁹ Y. Mikami,⁵⁸ K. Miyabayashi,³³ H. Miyake,⁴³ H. Miyata,³⁹ Y. Miyazaki,³¹ R. Mizuk,¹⁹ A. Moll,^{29,55} T. Mori,³¹ T. Müller,²² R. Mussa,¹⁸ T. Nagamine,⁵⁸ Y. Nagasaka,¹¹ Y. Nakahama,⁵⁹ I. Nakamura,¹⁰ E. Nakano,⁴² M. Nakao,¹⁰ H. Nakayama,⁵⁹ H. Nakazawa,³⁴ Z. Natkaniec,³⁷ K. Neichi,⁵⁷ S. Neubauer,²² S. Nishida,¹⁰ K. Nishimura,⁹ O. Nitoh,⁶² S. Noguchi,³³ T. Nozaki,¹⁰ A. Ogawa,⁴⁷ S. Ogawa,⁵⁶ T. Ohshima,³¹ S. Okuno,²¹ S. L. Olsen,⁵⁰ W. Ostrowicz,³⁷ H. Ozaki,¹⁰ P. Pakhlov,¹⁹ G. Pakhlova,¹⁹ H. Palka,³⁷ C. W. Park,⁵² H. Park,²⁵ H. K. Park,²⁵ K. S. Park,⁵² L. S. Peak,⁵³ M. Pernicka,¹⁵ R. Pestotnik,²⁰ M. Peters,⁹ L. E. Piilonen,⁶⁴ A. Poluektov,^{1,41} K. Prothmann,^{29,55} B. Riesert,²⁹ M. Rozanska,³⁷ H. Sahoo,⁹ K. Sakai,³⁹ Y. Sakai,¹⁰ N. Sasao,²⁴ O. Schneider,²⁶ P. Schönmeier,⁵⁸ J. Schümamm,¹⁰ C. Schwanda,¹⁵ A. J. Schwartz,³ R. Seidl,⁴⁷ A. Sekiya,³³ K. Senyo,³¹ M. E. Sevir,³⁰ L. Shang,¹⁴ M. Shapkin,¹⁶ V. Shebalin,^{1,41} C. P. Shen,⁹ H. Shibuya,⁵⁶ S. Shiizuka,³¹ S. Shinomiya,⁴³ J.-G. Shiu,³⁶ B. Shwartz,^{1,41} F. Simon,^{29,55} J. B. Singh,⁴⁴ R. Sinha,¹⁷ A. Sokolov,¹⁶ E. Solovieva,¹⁹ S. Stanič,⁴⁰ M. Starič,²⁰ J. Stypula,³⁷ A. Sugiyama,⁴⁸ K. Sumisawa,¹⁰ T. Sumiyoshi,⁶¹ S. Suzuki,⁴⁸ S. Y. Suzuki,¹⁰ Y. Suzuki,³¹ F. Takasaki,¹⁰ N. Tamura,³⁹ K. Tanabe,⁵⁹ M. Tanaka,¹⁰ N. Taniguchi,¹⁰ G. N. Taylor,³⁰ Y. Teramoto,⁴² I. Tikhomirov,¹⁹ K. Trabelsi,¹⁰ Y. F. Tse,³⁰ T. Tsuboyama,¹⁰ K. Tsunada,³¹ Y. Uchida,⁶ S. Uehara,¹⁰ Y. Ueki,⁶¹ K. Ueno,³⁶ T. Uglov,¹⁹ Y. Unno,⁸ S. Uno,¹⁰ P. Urquijo,³⁰ Y. Ushiroda,¹⁰ Y. Usov,^{1,41} G. Varner,⁹ K. E. Varvell,⁵³ K. Vervink,²⁶ A. Vinokurova,^{1,41} C. C. Wang,³⁶ C. H. Wang,³⁵ J. Wang,⁴⁵ M.-Z. Wang,³⁶ P. Wang,¹⁴ X. L. Wang,¹⁴ M. Watanabe,³⁹ Y. Watanabe,²¹ R. Wedd,³⁰ J.-T. Wei,³⁶ J. Wicht,¹⁰ L. Widhalm,¹⁵ J. Wiechczynski,³⁷ E. Won,²³ B. D. Yabsley,⁵³ H. Yamamoto,⁵⁸ Y. Yamashita,³⁸ M. Yamauchi,¹⁰ C. Z. Yuan,¹⁴ Y. Yusa,⁶⁴ C. C. Zhang,¹⁴ L. M. Zhang,⁴⁹ Z. P. Zhang,⁴⁹ V. Zhilich,^{1,41} V. Zhulanov,^{1,41} T. Zivko,²⁰ A. Zupanc,²⁰ N. Zwahlen,²⁶ and O. Zyukova,^{1,41}

(The Belle Collaboration)

¹*Budker Institute of Nuclear Physics, Novosibirsk*

²*Chiba University, Chiba*

³*University of Cincinnati, Cincinnati, Ohio 45221*

⁴*Department of Physics, Fu Jen Catholic University, Taipei*

⁵*Justus-Liebig-Universität Gießen, Gießen*

⁶*The Graduate University for Advanced Studies, Hayama*

⁷*Gyeongsang National University, Chinju*

⁸*Hanyang University, Seoul*

⁹*University of Hawaii, Honolulu, Hawaii 96822*

¹⁰*High Energy Accelerator Research Organization (KEK), Tsukuba*

¹¹*Hiroshima Institute of Technology, Hiroshima*

¹²*University of Illinois at Urbana-Champaign, Urbana, Illinois 61801*

¹³*Indian Institute of Technology Guwahati, Guwahati*

¹⁴*Institute of High Energy Physics, Chinese Academy of Sciences, Beijing*

¹⁵*Institute of High Energy Physics, Vienna*

- ¹⁶*Institute of High Energy Physics, Protvino*
¹⁷*Institute of Mathematical Sciences, Chennai*
¹⁸*INFN - Sezione di Torino, Torino*
¹⁹*Institute for Theoretical and Experimental Physics, Moscow*
²⁰*J. Stefan Institute, Ljubljana*
²¹*Kanagawa University, Yokohama*
²²*Institut für Experimentelle Kernphysik, Universität Karlsruhe, Karlsruhe*
²³*Korea University, Seoul*
²⁴*Kyoto University, Kyoto*
²⁵*Kyungpook National University, Taegu*
²⁶*École Polytechnique Fédérale de Lausanne (EPFL), Lausanne*
²⁷*Faculty of Mathematics and Physics, University of Ljubljana, Ljubljana*
²⁸*University of Maribor, Maribor*
²⁹*Max-Planck-Institut für Physik, München*
³⁰*University of Melbourne, School of Physics, Victoria 3010*
³¹*Nagoya University, Nagoya*
³²*Nara University of Education, Nara*
³³*Nara Women's University, Nara*
³⁴*National Central University, Chung-li*
³⁵*National United University, Miao Li*
³⁶*Department of Physics, National Taiwan University, Taipei*
³⁷*H. Niewodniczanski Institute of Nuclear Physics, Krakow*
³⁸*Nippon Dental University, Niigata*
³⁹*Niigata University, Niigata*
⁴⁰*University of Nova Gorica, Nova Gorica*
⁴¹*Novosibirsk State University, Novosibirsk*
⁴²*Osaka City University, Osaka*
⁴³*Osaka University, Osaka*
⁴⁴*Panjab University, Chandigarh*
⁴⁵*Peking University, Beijing*
⁴⁶*Princeton University, Princeton, New Jersey 08544*
⁴⁷*RIKEN BNL Research Center, Upton, New York 11973*
⁴⁸*Saga University, Saga*
⁴⁹*University of Science and Technology of China, Hefei*
⁵⁰*Seoul National University, Seoul*
⁵¹*Shinshu University, Nagano*
⁵²*Sungkyunkwan University, Suwon*
⁵³*School of Physics, University of Sydney, NSW 2006*
⁵⁴*Tata Institute of Fundamental Research, Mumbai*
⁵⁵*Excellence Cluster Universe, Technische Universität München, Garching*
⁵⁶*Toho University, Funabashi*
⁵⁷*Tohoku Gakuin University, Tagajo*
⁵⁸*Tohoku University, Sendai*
⁵⁹*Department of Physics, University of Tokyo, Tokyo*
⁶⁰*Tokyo Institute of Technology, Tokyo*
⁶¹*Tokyo Metropolitan University, Tokyo*
⁶²*Tokyo University of Agriculture and Technology, Tokyo*
⁶³*Toyama National College of Maritime Technology, Toyama*
⁶⁴*IPNAS, Virginia Polytechnic Institute and State University, Blacksburg, Virginia 24061*
⁶⁵*Yonsei University, Seoul*

We report the first observation of $B_s^0 \rightarrow J/\psi\eta$ and evidence for $B_s^0 \rightarrow J/\psi\eta'$. These results are obtained from 23.6 fb^{-1} of data collected at the $\Upsilon(5S)$ resonance with the Belle detector at the KEKB e^+e^- collider. We measure the branching fractions $\mathcal{B}(B_s^0 \rightarrow J/\psi\eta) = (3.32 \pm 0.87(\text{stat.})_{-0.28}^{+0.32}(\text{syst.}) \pm 0.42(f_s)) \times 10^{-4}$ with a significance of 7.3σ , and $\mathcal{B}(B_s^0 \rightarrow J/\psi\eta') = (3.1 \pm 1.2(\text{stat.})_{-0.6}^{+0.5}(\text{syst.}) \pm 0.38(f_s)) \times 10^{-4}$ with a significance of 3.8σ .

PACS numbers: 13.25.Hw, 14.40.Nd

The decays $B_s^0 \rightarrow J/\psi\eta^{(\prime)}$ are dominated by the $b \rightarrow c\bar{c}s$ process, as shown in Figure 1. The $J/\psi\eta^{(\prime)}$ final states are CP eigenstates, whose time distribution can be

used to measure directly the B_s^0 width difference $\Delta\Gamma_s$ [1]. Using SU(3) flavor symmetry, an estimate of the $B_s^0 \rightarrow J/\psi\eta^{(\prime)}$ branching fractions can be obtained relative to

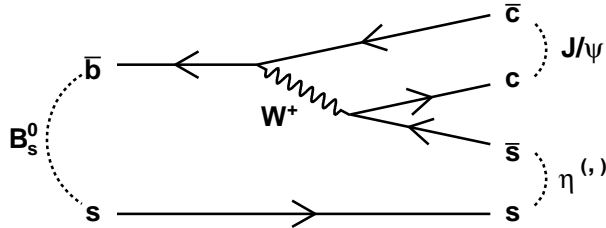


FIG. 1: Dominant diagram for the processes $B_s^0 \rightarrow J/\psi\eta^{(\prime)}$.

the decay $B_d^0 \rightarrow J/\psi K^0$ [2, 3]:

$$\frac{\mathcal{B}(B_s^0 \rightarrow J/\psi\eta^{(\prime)})}{\mathcal{B}(B_d^0 \rightarrow J/\psi K^0)} = \sin^2(\cos^2)\phi_P \times p_{B_s^0}^*/p_{B_d^0}^3,$$

where p^* is the momentum of J/ψ or $\eta^{(\prime)}$ in the rest frame of the B_s^0 or B_d^0 . Here, $\phi_P \simeq 37^\circ$ is the quark mixing angle in the flavor basis with $\eta = \frac{1}{\sqrt{2}}(u\bar{u} + d\bar{d})\cos\phi_P - s\bar{s}\sin\phi_P$. We then expect $\mathcal{B}(B_s^0 \rightarrow J/\psi\eta^{(\prime)}) \sim 3.45(4.88) \times 10^{-4}$, using the value $\mathcal{B}(B_d^0 \rightarrow J/\psi K^0) = 8.71 \times 10^{-4}$ [4]. To date there is only the upper limit $\mathcal{B}(B_s^0 \rightarrow J/\psi\eta) < 3.8 \times 10^{-3}$ at 90% confidence level [5]. Recently, a large sample of B_s^0 mesons was produced from e^+e^- collisions at the $\Upsilon(5S)$ resonance, where final states with photons can be reconstructed with low background.

In this letter, we report measurements of fully reconstructed $B_s^0 \rightarrow J/\psi\eta$ and $B_s^0 \rightarrow J/\psi\eta'$ decays using a $(23.6 \pm 0.3) \text{ fb}^{-1}$ data sample collected with the Belle detector at the KEKB asymmetric-energy e^+e^- collider [6] operated at the $\Upsilon(5S)$ resonance. The beam energy in the center-of-mass (CM) frame E_{beam} is measured to be $5433.5 \pm 0.5 \text{ MeV}$ using $\Upsilon(5S) \rightarrow \Upsilon(1S)\pi^+\pi^-$, $\Upsilon(1S) \rightarrow \mu^+\mu^-$ decays [8]. The total $b\bar{b}$ cross section at the $\Upsilon(5S)$ energy has been measured to be $\sigma_{b\bar{b}}^{\Upsilon(5S)} = (0.302 \pm 0.014) \text{ nb}$ [9]. B_s^0 events are produced from $B_s^{(*)}\bar{B}_s^{(*)}$ pairs where three B_s^0 production channels $B_s^0\bar{B}_s^0$, $B_s^*\bar{B}_s^0$, $B_s^*\bar{B}_s^*$ are kinematically allowed. The total fraction of $B_s^{(*)}\bar{B}_s^{(*)}$ pairs in $b\bar{b}$ events has been measured to be $f_s = N_{B_s^{(*)}\bar{B}_s^{(*)}}/N_{b\bar{b}} = (19.5_{-2.3}^{+3.0})\%$ [9]. Thus, the 23.6 fb^{-1} data sample contains a total of 2.78 million B_s^0 mesons. The fractions of B_s^0 production channels are measured to be $f_{B_s^*\bar{B}_s^*} = N_{B_s^*\bar{B}_s^*}/N_{B_s^{(*)}\bar{B}_s^{(*)}} = (90.1_{-4.0}^{+3.8} \pm 0.2)\%$, $f_{B_s^*\bar{B}_s^0} = N_{B_s^*\bar{B}_s^0}/N_{B_s^{(*)}\bar{B}_s^{(*)}} = (7.3_{-0.30}^{+0.33} \pm 0.1)\%$ [10].

The Belle detector is a large-solid-angle magnetic spectrometer that consists of a silicon vertex detector (SVD), a 50-layer central drift chamber (CDC), an array of aerogel threshold Cherenkov counters (ACC), a barrel-like arrangement of time-of-flight scintillation counters (TOF), and an electromagnetic calorimeter (ECL) comprised of CsI(Tl) crystals located inside a superconduct-

ing solenoid coil that provides a 1.5 T magnetic field. An iron flux-return located outside the coil is instrumented to detect K_L^0 mesons and identify muons (KLM). The detector is described in detail elsewhere [7].

Charged tracks are required to originate within 0.5 cm in the radial direction and within 5 cm in the beam direction, with respect to the interaction point. Electron candidates are identified by combining information from the ECL, the CDC (dE/dx), and the ACC. Muon candidates are identified through track penetration depth and hit patterns in the KLM system. Identification of pions is based on combining information from the CDC (dE/dx), the TOF and the ACC.

Two oppositely charged leptons l^+l^- ($l = e$ or μ) and bremsstrahlung photons lying within 50 mrad of e^+ or e^- tracks are combined to form a J/ψ meson. The leptons are required to be positively identified as electrons or muons. The invariant mass is required to lie in the ranges $-0.150 \text{ GeV}/c^2 < M_{ee(\gamma)} - m_{J/\psi} < 0.036 \text{ GeV}/c^2$ and $-0.060 \text{ GeV}/c^2 < M_{\mu\mu} - m_{J/\psi} < 0.036 \text{ GeV}/c^2$, where $m_{J/\psi}$ denotes the nominal J/ψ mass, and $M_{ee(\gamma)}$ and $M_{\mu\mu}$ are the reconstructed invariant masses for $e^+e^-(\gamma)$ and $\mu^+\mu^-$, respectively.

Photon candidates are selected from ECL showers not associated with charged tracks. An energy deposition with a photon-like shape and an energy greater than 50 MeV is required. π^0 candidates are selected by combining two photon candidates with an invariant mass in the range $115 \text{ MeV}/c^2 < M_{\gamma\gamma} < 155 \text{ MeV}/c^2$.

Candidate η mesons are reconstructed in the $\gamma\gamma$ and $\pi^+\pi^-\pi^0$ final states. We require the invariant mass to be in the range $500 \text{ MeV}/c^2 < M_{\gamma\gamma} < 575 \text{ MeV}/c^2$ ($[-3.5\sigma, 2.0\sigma]$) and $535 \text{ MeV}/c^2 < M_{\pi^+\pi^-\pi^0} < 560 \text{ MeV}/c^2$ ($\pm 2.5\sigma$). In the $\gamma\gamma$ final state, we require that $|\cos\theta_{\text{dec}}| < 0.9$, to reduce background from combinatorial γ 's, where θ_{dec} is the angle between the γ and η lab momentum direction in the η rest frame.

Candidate η' mesons are reconstructed in the $\eta\pi^+\pi^-$ and $\rho^0\gamma$ channels. The η candidates are selected in the same two channels as above. Thus, there are three sub-channels for η' reconstruction. ρ^0 's are selected from oppositely charged pion pairs satisfying $550 \text{ MeV}/c^2 < M_{\pi^+\pi^-} < 900 \text{ MeV}/c^2$ and a helicity requirement $|\cos\theta_{\text{hel}}| < 0.85$ since the ρ^0 is longitudinally polarized. Here θ_{hel} is the helicity angle of ρ^0 , calculated as the angle between the direction of the π^+ and the direction opposite to the η' momentum in the ρ^0 rest frame. We require the reconstructed η' invariant mass to satisfy $940 \text{ MeV}/c^2 < M_{\eta'} < 975 \text{ MeV}/c^2$ ($\pm 3\sigma$).

We combine J/ψ and $\eta^{(\prime)}$ candidates to form B_s^0 mesons. Signal candidates are identified by two kinematic variables computed in the $\Upsilon(5S)$ frame: the energy difference $\Delta E = E_B^* - E_{\text{beam}}$ and the beam-energy constrained mass $M_{\text{bc}} = \sqrt{(E_{\text{beam}})^2 - (p_B^*)^2}$, where E_B^* and p_B^* are the energy and momentum of the reconstructed B_s^0 candidate. To improve the ΔE and M_{bc} resolutions,

mass-constrained kinematic fits are applied to J/ψ , $\eta^{(\prime)}$ and π^0 candidates. We retain B_s^0 meson candidates with $|\Delta E| < 0.4$ GeV and $M_{bc} > 5.25$ GeV/ c^2 for further analysis. If there are multiple candidates in a single event, we choose the candidate that minimizes the sum of the χ^2 's of the mass-constrained fits.

To suppress the two-jet-like continuum background from $e^+e^- \rightarrow q\bar{q}$ ($q = u, d, s, c$), we require the ratio of second to zeroth Fox-Wolfman moments [11] to be less than 0.4. This requirement is optimized by maximizing a figure-of-merit $N_S/\sqrt{N_S + N_B}$, where N_S is the expected number of signal events and N_B is the number of continuum events, in the $B^*\bar{B}^*$ signal region. The continuum background is modeled by a second-order polynomial in ΔE and an ARGUS function [12] in M_{bc} . We study the continuum background in a J/ψ sideband defined as 2.5 GeV/ $c^2 < M_{J/\psi} < 3.4$ GeV/ c^2 , excluding the region $-0.200(-0.080)$ GeV/ $c^2 < M_{J/\psi} - m_{J/\psi} < 0.048$ GeV/ c^2 for $J/\psi \rightarrow e^+e^-(\mu^+\mu^-)$ in data. The shapes for continuum backgrounds for each sub-channel are determined from fits to J/ψ sideband data with a relaxed lepton identification requirement. The yields for continuum background are determined from the yields in J/ψ sideband data with all selections other than the J/ψ mass cut as in the nominal selection. Scale factors are determined from the ratio of the J/ψ selection area to the J/ψ sideband area by fitting Monte Carlo (MC) J/ψ mass distributions. For continuum J/ψ backgrounds that may not be well modeled in MC, we studied the off-resonance data and obtained the fractions of real J/ψ 's in continuum, which are applied as a correction to the continuum background yields.

The remaining background is from $B\bar{B}$ ($B = B_s^0, B_d^0, B_u^\pm$) events with one B meson decays to a final state with J/ψ (denoted $J/\psi X$). We use a MC sample generated at the $\Upsilon(5S)$ resonance that includes all known $B \rightarrow J/\psi X$ processes to estimate this background, and find that the dominant contribution is from $B_d^0, B_u^\pm \rightarrow J/\psi +$ strange mesons. This background does not peak in either ΔE and M_{bc} and is described by an exponential function in ΔE and an ARGUS function in M_{bc} , with shapes determined from MC. For the channel $J/\psi\eta'(\rho^0\gamma)$, the size of the $J/\psi X$ background is comparable to the expected signal yield in the $B_s^*\bar{B}_s^*$ signal region, so we use a η' sideband defined as 0.90 GeV/ $c^2 < M_{\eta'} < 0.93$ GeV/ c^2 and 0.99 GeV/ $c^2 < M_{\eta'} < 1.02$ GeV/ c^2 to study it. We fit the η' sideband data to obtain the $J/\psi X$ background shape for the $J/\psi\eta'(\rho^0\gamma)$ channel, where the continuum contribution is fixed from the J/ψ sideband.

We categorize events into two η and three η' sub-channels. For the $J/\psi\eta$ and $J/\psi\eta'$ modes, we perform a simultaneous unbinned maximum likelihood fit to the $\Delta E - M_{bc}$ distributions for each group of two η or three η' sub-channels, with the signal branching fraction as a common parameter while treating the signal

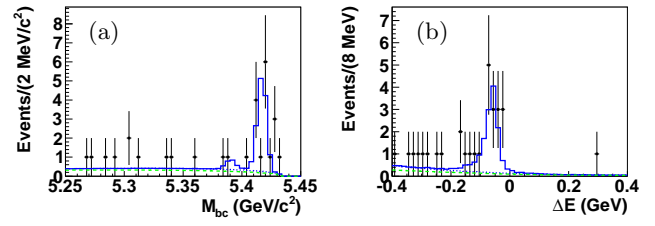


FIG. 2: Distributions for the $B_s^*\bar{B}_s^*$ signal region with $\Delta E \in [-97, -9]$ MeV, and (b) ΔE distribution for the $B_s^*\bar{B}_s^*$ signal region with $M_{bc} \in [5.405, 5.431]$ GeV/ c^2 . The full histogram shows projections of fit results. The sum of all backgrounds is represented by the blue dotted curves with the green dashed curve corresponding to continuum background.

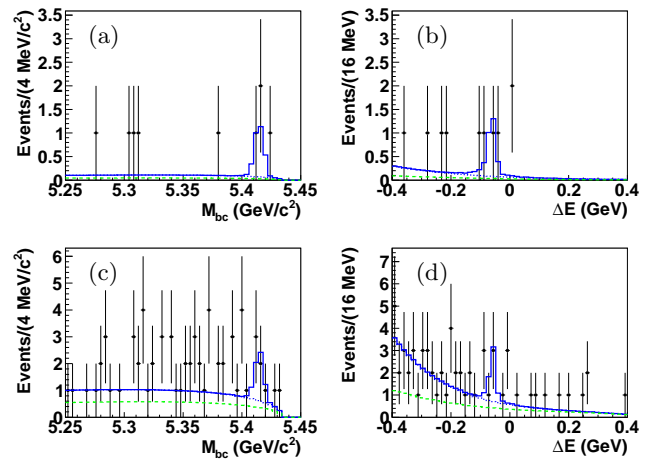


FIG. 3: Fit projections for the combined clean $J/\psi\eta'(\eta\pi^+\pi^-)$ channels (a,b) and $J/\psi\eta'(\rho^0\gamma)$ channel (c,d). The projections are shown in the $B_s^*\bar{B}_s^*$ signal region with $\Delta E \in [-98, -17]$ MeV (a,c), and with $M_{bc} \in [5.403, 5.428]$ GeV/ c^2 (b,d). The sum of all backgrounds is represented by the blue dotted curves with the green dashed curve corresponding to continuum background.

and background shapes separately for the different $\eta^{(\prime)}$ sub-channels.

In the fit, the signal normalization for each B_s^0 production channel is parameterized as $N_{\text{sig}} = 2 \times N_{B_s^{(*)}\bar{B}_s^{(*)}} f_{B_s^{(*)}\bar{B}_s^{(*)}} \mathcal{B}(B_s^0 \rightarrow J/\psi\eta^{(\prime)}) \Sigma_i \mathcal{B}_i \epsilon_i$. We use three fractions $f_{B_s^*\bar{B}_s^*}$, $f_{B_s^*\bar{B}_s^0}$, and $f_{B_s^0\bar{B}_s^0} = 1 - f_{B_s^*\bar{B}_s^*} - f_{B_s^*\bar{B}_s^0}$. In the $J/\psi\eta'$ mode, because of low statistics, we only include the $B_s^*\bar{B}_s^*$ channel in the fit. The index i denotes each $\eta^{(\prime)}$ sub-channel. The product $\mathcal{B}_i = \mathcal{B}(J/\psi \rightarrow l^+l^-) \mathcal{B}_i(\eta^{(\prime)})$ is the total branching fraction to final states with a J/ψ and an $\eta^{(\prime)}$, and ϵ_i is the MC reconstruction efficiency. The values of the weighted efficiencies $\mathcal{B}_i \epsilon_i$ are listed in Table I. The signal shapes are from signal MC histograms while the means and widths of the distributions are corrected using a $B^+ \rightarrow J/\psi K^{*+}(K^{*+} \rightarrow K^+\pi^0)$ control sample from $\Upsilon(4S)$. The continuum back-

TABLE I: A summary of efficiencies, significances and branching fractions (\mathcal{B}) for each mode.

mode	$\mathcal{B}_i \epsilon_i$	Significance	\mathcal{B}
$B_s^0 \rightarrow J/\psi\eta(\gamma\gamma)$	1.34%		
$B_s^0 \rightarrow J/\psi\eta(\pi^+\pi^-\pi^0)$	0.45%		
Total $B_s^0 \rightarrow J/\psi\eta$	1.79%	7.3σ	$(3.32 \pm 0.87(\text{stat.})_{-0.28}^{+0.32}(\text{syst.}) \pm 0.42(f_s)) \times 10^{-4}$
$B_s^0 \rightarrow J/\psi\eta'(\eta\pi\pi)$	0.52%		
$B_s^0 \rightarrow J/\psi\eta'(\rho^0\gamma)$	0.88%		
Total $B_s^0 \rightarrow J/\psi\eta'$	1.40%	3.8σ	$(3.1 \pm 1.2(\text{stat.})_{-0.6}^{+0.5}(\text{syst.}) \pm 0.38(f_s)) \times 10^{-4}$

TABLE II: Relative systematic errors (in %) for $\mathcal{B}(J/\psi\eta^{(\prime)})$.

Source	$\mathcal{B}(J/\psi\eta)$	$\mathcal{B}(J/\psi\eta')$
Signal shape calibration	+5.8, -2.9	+11.7, -16.8
Beam energy	+1.6, -0.0	+4.8, -4.3
MC signal shape	+1.0, -2.0	+2.6, -4.0
$f_{B_s^{(*)}\bar{B}_s^{(*)}}$	+0.7, -1.5	+4.6, -4.0
Background parameters	+0.9, -0.8	+6.0, -5.5
Track reconstruction	2.5	4.2
Lepton identification	4.2	4.1
Pion identification	0.4	2.3
$\eta(\pi^0) \rightarrow \gamma\gamma$ selection	4.1	2.8
$\mathcal{B}(J/\psi \rightarrow ll)$	0.72	0.72
$\mathcal{B}(\eta^{(\prime)} \rightarrow \text{final states})$	0.49	2.3
Luminosity	1.3	1.3
$\sigma_{b\bar{b}}$	4.6	4.6
f_s	+13.4, -13.3	+13.4, -13.3
Total	+16.8, -16.1	+21.9, -24.8

ground's shapes and yields and the $J/\psi X$ background's shapes are fixed. The floating parameters for each fit are the branching fraction $\mathcal{B}(B_s^0 \rightarrow J/\psi\eta^{(\prime)})$ and the $J/\psi X$ background yields for each sub-channel.

The projections of the fit in the $B_s^* \bar{B}_s^*$ signal region are shown in Figures 2 and 3. The signal efficiencies, branching fractions, and significances including systematic uncertainties are listed in Table I. We calculate a total of $14.9 \pm 4.1 B_s^0 \rightarrow J/\psi\eta$ events and $10.7 \pm 4.6 B_s^0 \rightarrow J/\psi\eta'$ events in the $\Upsilon(5S) \rightarrow B_s^* \bar{B}_s^*$ channel.

The $B_s^0 \rightarrow J/\psi\eta$ decay is observed for the first time and evidence for the $B_s^0 \rightarrow J/\psi\eta'$ decay is found. The significance is defined by $S = \sqrt{2 \ln(\mathcal{L}_{\text{max}}/\mathcal{L}_0)}$, where $\mathcal{L}_{\text{max}}(\mathcal{L}_0)$ is the likelihood value at the maximum (with the signal branching fraction set to zero). The significance including systematic uncertainty is taken as the smallest value for each systematic variation described below.

The muon and pion identification efficiencies from MC are calibrated using the $J/\psi \rightarrow l^+l^-$ and $D^{*+} \rightarrow D^0\pi^+$ control samples in data, respectively. The total systematic error due to lepton identification is weighted to be

4.2(4.1)% for $J/\psi\eta^{(\prime)}$ modes. The systematic error due to pion identification is 0.4(2.3)% for the $J/\psi\eta^{(\prime)}$ modes.

The systematic errors due to the signal shape mean and width corrections and background parameters are determined by varying each parameter by its error, repeating the fit, and summing the shifts in branching fraction in quadrature. The beam energy has an error of ± 0.5 MeV, whose systematic effect is evaluated by varying the mean value of ΔE and M_{bc} for the signal shapes simultaneously according to the uncertainty in the beam energy. All the systematic errors are summarized in Table II. The large systematic errors due to f_s are quoted separately in the final results.

The ratio of the two branching fractions $R = \mathcal{B}(B_s^0 \rightarrow J/\psi\eta')/\mathcal{B}(B_s^0 \rightarrow J/\psi\eta)$ is also calculated. The statistical errors of the two modes are combined. The common systematic errors due to luminosity, cross-section and f_s cancel. Correlated systematic errors due to calibration, beam energy, track reconstruction and particle identification are treated properly by varying the numerator and denominator simultaneously. Other systematic sources in the two branching fractions are treated independently.

In summary, we observe $B_s^0 \rightarrow J/\psi\eta$ decay with a significance of 7.3σ and find evidence for $B_s^0 \rightarrow J/\psi\eta'$ with a significance of 3.8σ . We measure the branching fractions $\mathcal{B}(B_s^0 \rightarrow J/\psi\eta) = (3.32 \pm 0.87(\text{stat.})_{-0.28}^{+0.32}(\text{syst.}) \pm 0.42(f_s)) \times 10^{-4}$ and $\mathcal{B}(B_s^0 \rightarrow J/\psi\eta') = (3.1 \pm 1.2(\text{stat.})_{-0.6}^{+0.5}(\text{syst.}) \pm 0.38(f_s)) \times 10^{-4}$. The ratio of two branching fractions is measured as $R = \frac{\mathcal{B}(B_s^0 \rightarrow J/\psi\eta')}{\mathcal{B}(B_s^0 \rightarrow J/\psi\eta)} = 0.924_{-0.44}^{+0.52}(\text{stat.})_{-0.20}^{+0.15}(\text{syst.})$. The results are consistent with SU(3) expectations using the measured value of $\mathcal{B}(B_d^0 \rightarrow J/\psi K^0)$ [2, 3].

We thank the KEKB group for excellent operation of the accelerator, the KEK cryogenics group for efficient solenoid operations, and the KEK computer group and the NII for valuable computing and SINET3 network support. We acknowledge support from MEXT, JSPS and Nagoya's TLPFC (Japan); ARC and DIISR (Australia); NSFC (China); DST (India); MEST, KOSEF, KRF (Korea); MNiSW (Poland); MES and RFAAE (Russia); ARRS (Slovenia); SNSF (Switzerland); NSC and MOE (Taiwan); and DOE (USA).

* now at Okayama University, Okayama

- [1] I. Dunietz, R. Fleischer and U. Nierste, *Phys. Rev. D* **63**, 114015 (2001) [arXiv:hep-ph/0012219].
- [2] P. Z. Skands, *JHEP* **0101**, 008 (2001) [arXiv:hep-ph/0010115].
- [3] C. E. Thomas, *JHEP* **0710**, 026 (2007) [arXiv:0705.1500 [hep-ph]].
- [4] C. Amsler *et al.* [Particle Data Group], *Phys. Lett. B* **667**, 1 (2008).
- [5] M. Acciarri *et al.* [L3 Collaboration], *Phys. Lett. B* **391**, 481 (1997).
- [6] S. Kurokawa and E. Kikutani, *Nucl. Instr. and Meth. A* **499**, 1 (2003).
- [7] A. Abashian *et al.* [Belle Collaboration], *Nucl. Instrum. Meth. A* **479**, 117 (2002).
- [8] K. F. Chen *et al.* [Belle Collaboration], *Phys. Rev. Lett.* **100**, 112001 (2008) [arXiv:0710.2577 [hep-ex]].
- [9] A. Drutskoy *et al.* [Belle Collaboration], *Phys. Rev. Lett.* **98**, 052001 (2007), G. S. Huang *et al.* [CLEO Collaboration], *Phys. Rev. D* **75**, 012002 (2007). We are using the $\sigma_{b\bar{b}}^{\Upsilon(5S)}$ value, 0.302 ± 0.014 nb, which is an average of these two measurements.
- [10] R. Louvot *et al.* [Belle Collaboration], *Phys. Rev. Lett.* **102**, 021801 (2009) [arXiv:0809.2526 [hep-ex]].
- [11] The Fox-Wolfram moments were introduced in G. C. Fox and S. Wolfram, *Phys. Rev. Lett.* **41**, 1581 (1978).
- [12] H. Albrecht *et al.* [ARGUS Collaboration], *Phys. Lett. B* **185**, 218 (1987).